Recent Advances in Semiconductor Nanowire Lasers

Samuel W. Eaton,[1†] Anthony Fu,[1,2†] Andrew B. Wong,[1,2] C.Z. Ning,[3,4] Peidong Yang[1,2,5,6]*

The discovery and continued development of the laser has revolutionized both science and industry, enabling a range of scientific advances. The advent of miniaturized, semiconductor lasers has made this technology ubiquitous and an integral part of everyday life. Exciting research continues with a new focus on nanowire lasers, as they have the potential to revolutionize the field of optoelectronics. Here, we review the latest advancements in nanowire laser development and offer our perspective on future improvements and trends. We discuss fundamental material considerations, which include the latest, most effective materials for nanowire lasers. A discussion of novel cavity designs and amplifications methods is followed by some of the latest work on surface plasmon polariton nanowire lasers. Finally, exciting new reports of electrically pumped nanowire lasers with the potential for integrated optoelectronic applications are described.

[1] Department of Chemistry, University of California, Berkeley, California 94720, USA.

[2] Materials Sciences Division, Lawrence Berkeley National Laboratory, Berkeley, CA 94720, USA.

[3] School of Electrical, Computer and Energy Engineering, Arizona State University, Tempe, AZ 85287, USA.

[4] Department of Electronic Engineering, Tsinghua University, Beijing, China.

[5] Kavli Energy NanoSciences Institute, Berkeley, California 94720, USA.

[6] Department of Materials Science and Engineering, University of California, Berkeley, CA 94720, USA.

[†]These authors contributed equally.

*Corresponding author. E-mail: p_yang@berkeley.edu (P.Y.)

Introduction

In 1916, Albert Einstein theorized the reciprocal nature of stimulated emission and absorption, which provided the underpinnings of lasing action.[1] Expanding on these principles, Charles Townes and Arthur Schawlow laid the foundation[2] for Theodore Maiman to demonstrate the first working laser using a ruby gain medium.[3] Since that time, the laser has branched into many sub-fields and evolved considerably with innovations in materials, optics, and electronics. The addition of new functionalities and improved properties has precipitated the emergence of new industries and the growth of existing industries (Figure 1). Lasers have a wide range of medical, commercial, and consumer applications making them widely viewed as a general purpose technology.[4,5]

Throughout this revolutionary period, there has been an intense interest in the miniaturization of the laser. The advent of compact semiconductor lasers has fundamentally changed the pace and nature of miniaturization and enabled the development of new technologies such as optical fiber communications, image scanning, compact disk players, barcode scanners, laser printers, and compact LIDAR systems.[6] Recently, the push for shrinking lasers has provided devices such as vertical-cavity surface-emitting lasers (VCSELs),[7] microdisk lasers,[8] and photonic crystal (PC) lasers,[9] some of which are used commercially. While miniaturization has allowed widespread adoption of lasers, the next frontier in laser research lies ahead. In the last decade, academic research has increasingly focused on exploring and developing nanoscale lasers for applications in on-chip photonic devices[10] and ultrasensitive sensors.[11] One of the principal areas of research in this field is the semiconductor nanowire: a quasi-one-dimensional semiconductor that simultaneously acts as an optical gain medium and optical cavity that, in some cases, can possess the intrinsic capability to lase.[10,12,13] This property, along with the ability to tune the emission wavelength and its potential for electrical integration, makes nanowire lasers promising candidates for use in the next generation of optoelectronic devices. This article seeks to introduce the reader to the concept of the nanowire laser, to relate the fundamental discoveries of the field, to review important, recent advances, and to offer a perspective on future research directions.
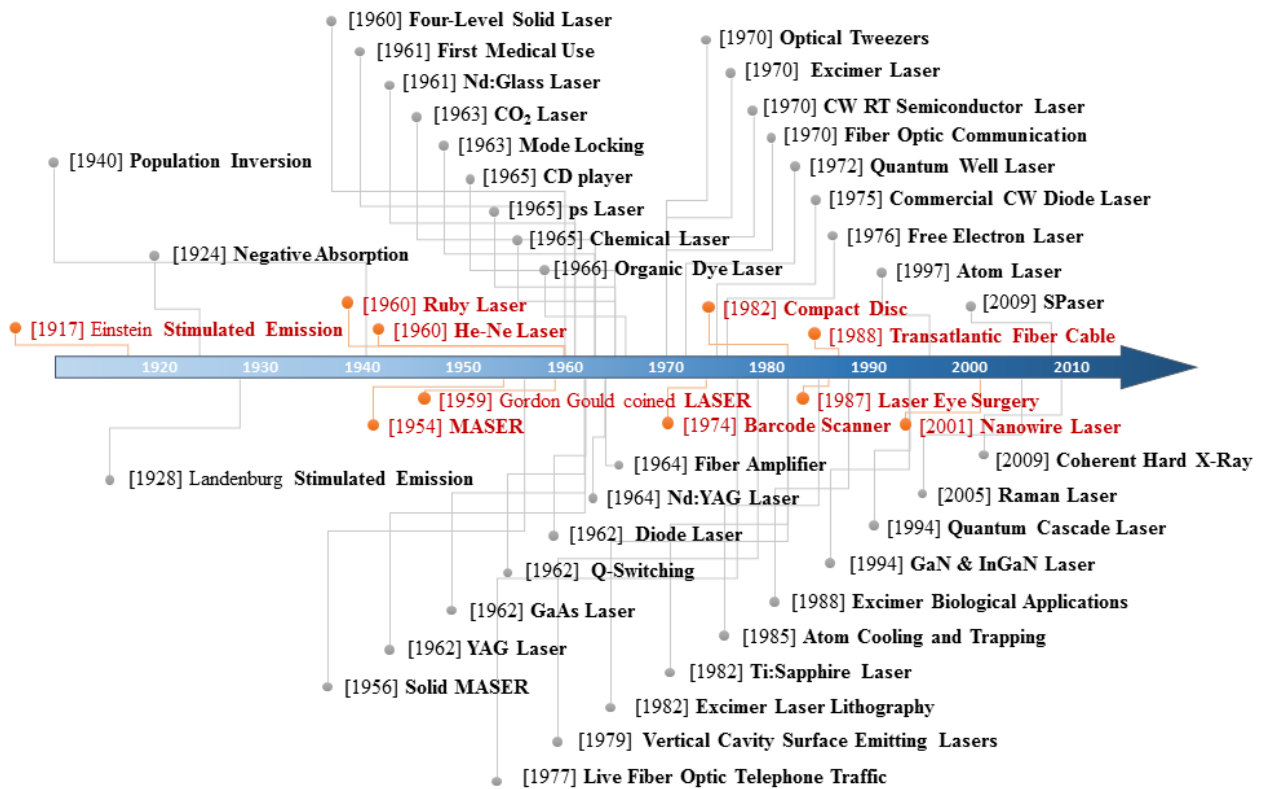
[1960] Four-Level Solid Laser
[1961] First Medical Use
[1961] Nd:Glass Laser
[1963] CO_2 Laser
[1963] Mode Locking
[1965] CD player
[1965] ps Laser
[1965] Chemical Laser
[1966] Organic Dye Laser

[1970] Optical Tweezers
[1970] Excimer Laser
[1970] CW RT Semiconductor Laser
[1970] Fiber Optic Communication
[1972] Quantum Well Laser
[1975] Commercial CW Diode Laser
[1976] Free Electron Laser
[1997] Atom Laser
[2009] SPaser

[1940] Population Inversion

[1924] Negative Absorption

[1960] Ruby Laser
[1960] He-Ne Laser

[1982] Compact Disc

[1917] Einstein Stimulated Emission
[1988] Transatlantic Fiber Cable

1920 1930 1940 1950 1960 1970 1980 1990 2000 2010

[1959] Gordon Gould coined LASER
[1987] Laser Eye Surgery
[1954] MASER
[1974] Barcode Scanner
[2001] Nanowire Laser

[1928] Landenburg Stimulated Emission
[1964] Fiber Amplifier
[2009] Coherent Hard X-Ray
[1964] Nd:YAG Laser
[2005] Raman Laser
[1962] Diode Laser
[1994] Quantum Cascade Laser
[1962] Q-Switching
[1994] GaN & InGaN Laser
[1962] GaAs Laser
[1988] Excimer Biological Applications
[1962] YAG Laser
[1985] Atom Cooling and Trapping
[1956] Solid MASER
[1982] Ti:Sapphire Laser
[1982] Excimer Laser Lithography
[1979] Vertical Cavity Surface Emitting Lasers
[1977] Live Fiber Optic Telephone Traffic

Figure 1. A brief timeline of laser discovery and development.

Nanowire Laser Fundamentals

The first semiconductor nanowires were grown from silicon using a vapor-liquid-solid growth mechanism, which utilized a gold metal catalyst to facilitate one-dimensional, crystalline growth.[14] Using this vapor-liquid-solid approach, the Yang group grew dense arrays of ZnO nanowires and reported the first observation of laser action from these synthesized nanowires.[15] This breakthrough introduced a novel and facile approach to the fabrication of nanoscale lasers (Figure 2). In contrast to traditional "top-down" fabrication techniques that etch macroscopic crystals to define nanoscale dimensions, these nanowire structures were grown on sapphire substrates coated with gold from the "bottom-up" by simply heating a mixture of ZnO and graphite in an argon atmosphere.[16] The natural anisotropy and the associated facets of the wurtzite structure of ZnO helped to define the optical cavity.

Although this demonstration represented a breakthrough in the miniaturization of the semiconductor laser, there remained several unanswered questions. It was postulated that the nanowire acts as a Fabry–Pérot cavity, but there was limited experimental evidence to support this claim. The first report was performed on an ensemble of nanowires with diameters varying

between 20-150 nm and lengths between 2-10 μm. This measurement produced a spectrum with the characteristics of individual nanowires averaged out over many nanowires. To further understand the properties of the cavity, single nanowires were obtained by sonication of an array of nanowires grown on a sapphire substrate in ethanol followed by drop-casting the solution onto a new substrate. Near-field scanning optical microscopy (NSOM) was used to examine the spatially resolved photoluminescence of these nanowires when excited above the lasing threshold.[17,18] This technique revealed that the emission intensity from the ends of the nanowire were much stronger than from the side facets of the nanowire and that the end facet emission of the nanowire displayed strong lasing peaks. Furthermore, the far-field spectra of these nanowires excited above their respective lasing threshold could be fit to the modes of a Fabry–Pérot cavity matching the nanowire length and could be related to more detailed theoretical simulations.[19]

Before the discovery of lasing in nanowire arrays, it was unclear if cavities with such small end facets could support lasing because it was thought they might induce substantial scattering losses and render the cavity too inefficient to reach the lasing threshold.[10] Amplification in a nanowire Fabry–Pérot cavity relies on optical feedback from light reflecting off of the crystalline end facets of the nanowire and back through the gain medium. Lasing is achieved when the round-trip gain exceeds the round-trip losses,[20,21]

$$\Gamma g > \alpha_m + \alpha_p = \frac{1}{2L} ln\left(\frac{1}{R_1 R_2}\right) + \alpha_p$$

where Γ is the confinement factor, g is the material gain, α_m is the mirror loss, α_p is the propagation loss, L is the cavity length, and R_1 and R_2 are the effective reflection coefficients for each end facet, which are nominally equal. As shown on the right side of the equation, end facet reflection efficiency plays a large role in determining mirror loss and the amount of gain required to reach the lasing threshold. When the nanowires have diameters that are on the order of the wavelength of light, the typical reflection process at a semiconductor-air interface becomes a scattering process. It has been shown theoretically that this "effective reflection" due to scattering at the end of a nanowire can be very different and, in some cases, much greater than the prediction of the standard Fresnel formulae, which provides the potential for decreased mirror loss.[22]

Another uncertainty encountered during the development of nanowire lasers was that it was unclear how much round-trip gain could be produced to compensate for mirror losses because nanowires are orders of magnitude shorter in length than conventional semiconductor laser cavities. The confinement factor, typically defined as the ratio of optical energy inside the gain medium to that in the total guided mode, offered a possible answer and ultimately embodies another advantageous aspect of the nanowire laser.[23,24] It has been suggested theoretically that the confinement factor in a nanowire laser could be larger than unity.[23] This property has been related to the strongly wave guiding nature of the nanowire, where the actual length of wave propagation may exceed the axial length of the nanowire.[24] A larger than unity confinement factor suggests that modal gain, amplification specific to a given mode, in addition to material gain may play a role in allowing a nanowire laser to reach the lasing threshold. In practice, this property may aid nanowire lasers in achieving lasing when it might not be possible for a different cavity geometry.
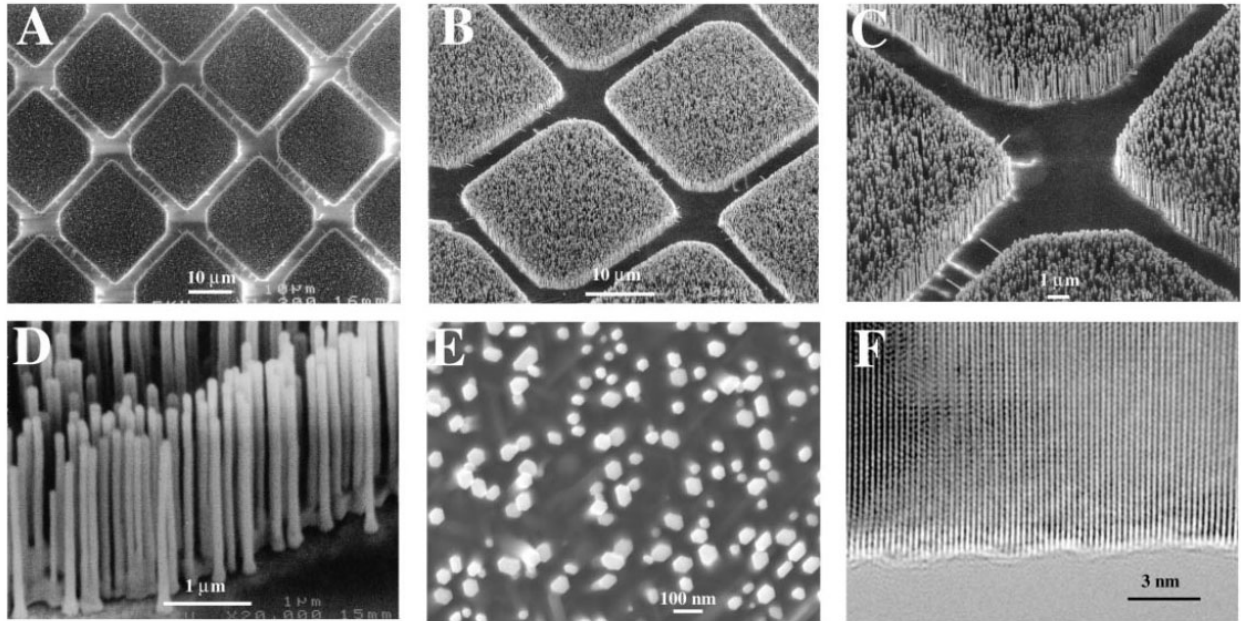
As the study of single-nanowire lasers matured, it has become increasingly important to rigorously model the nanoscale laser. Modeling helps define the lasing threshold, which can be

thought of as the amount of excitation necessary to turn the laser "on". Specifically, modeling the transition from amplified spontaneous emission (ASE) to lasing oscillation enables a closer examination of the threshold behavior. When lasers shrink in mode volume, the definition of the lasing threshold becomes less clear.[25] This threshold is generally shown in a power plot describing the relationship between the input excitation and the output emission. For a nanoscale laser, the lasing threshold is less distinguished because a larger fraction of the spontaneous emission is coupled into the laser mode. A rate equation analysis to model this relationship helps to define the threshold of nanowire lasers. The coupled rate equations to describe the carrier density and photon density for a single mode in a semiconductor cavity can be defined as

$$\frac{dN}{dt} = \eta P - \frac{N}{\tau_r} - \frac{N}{\tau_{nr}} - \Gamma a(N - N_0)S$$

$$\frac{dS}{dt} = \beta \frac{N}{\tau_r} + \Gamma a(N - N_0)S - \frac{1}{\tau_s}S$$

where N is the carrier density, S is the photon density, P is the pump intensity, η is the pumping efficiency, τ_r and τ_{nr} are the spontaneous emission and non-radiative lifetime, respectively, τ_s is the photon lifetime, β is the spontaneous emission factor, N_0 is the transparency carrier density, a is the differential gain, and Γ is the confinement factor. The gain is approximated in the linear regime by

$$g = a(N - N_0)$$

By solving for these coupled rate equations under steady state conditions, the photon density can be plotted as a function of pump intensity as shown in Figure 3 for various values of β. In this example, the numerical values for a, τ_s, τ_r, τ_{nr}, Γ, and N_0 used to construct this plot are from modeling GaN nanowire lasers.[26] The β value describes the fraction of spontaneous emission that couples into the laser mode of interest. In general, as the cavity volume shrinks, this spontaneous emission factor increases, and the threshold "softens," making the transition to lasing less abrupt.[25,27] By fitting the experimental power plot to a calculated plot, the lasing threshold can be more quantitatively defined. Furthermore, by plotting the output power against

the pumping power on a log-log scale, the change of the slope of the "S" curve demonstrates a lasing threshold transition, where the "super-linear" regime is often associated with the threshold.[20,21,28] Notably, when $\beta = 1$ and τ_{nr} is large compared to τ_r, the "S" curve becomes a straight line and lasing is seemingly "thresholdless" (Figure 3, purple trace). A recently reported examination of the quantum statistics suggests that, even without a distinct threshold in the input versus output plot, a finite threshold may be determined.[29] Qualitatively, the slope of the "S" curve may also help to identify false positives in experiments, which include a nonlinear sensitivity in the detector, insufficient data, or the exclusive observation of ASE. In general, the quantification of the lasing threshold is always preferable. It should also be noted that β may be overestimated in the fit depending on the experimental conditions. For example, in the case of a nanowire laying flat on a substrate, a significant fraction of the emission will not be collected during the experiment. Since lasing emission is more anisotropic than spontaneous emission, the collection scheme may lead to a slight overestimation of β.
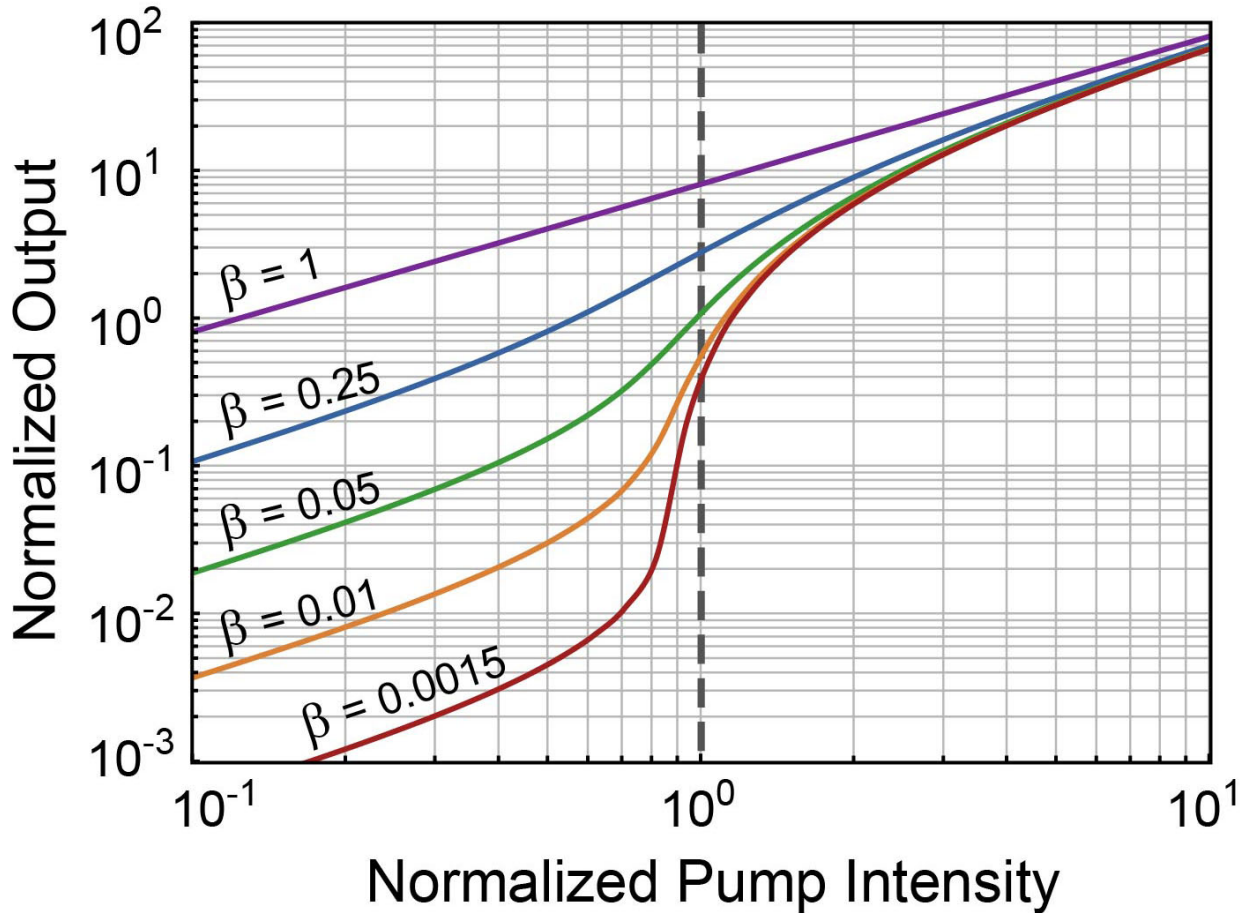
Figure 3. Calculated power plot of a hypothetical laser with different values of β. The pump intensity is normalized to the lasing threshold.

Semiconductor Materials for Nanowire Lasers

Since its first demonstration, the bottom-up synthesis of semiconductor nanowires with high optical quality has generated tremendous interest in the nano-material community because of a number of potential advantages over the fabrication of nano-lasers using conventional top-down techniques. The first of these advantages is that top-down techniques tend to require long and rigorous steps, which can potentially result in elevated costs. In addition, extensive fabrication expertise and great care are required to produce the high quality, nano-scale structures required for successful lasing. In comparison, chemical synthesis of nanostructures can be relatively simple and less time consuming. For example, in the case of ZnO nanowires, the synthesis can take 5-30 minutes after preparation.[16] Another advantage, which has been explored extensively, is that bottom-up synthetic techniques introduce new possibilities for the material composition of the nanowire laser. For example, some semiconductors, such as ZnO and CdS, are traditionally difficult materials to handle using conventional cleanroom techniques. This methodology for the chemical synthesis of nanowire lasers has allowed the exploration of numerous new materials. In fact, the use of relatively simple tube furnaces to grow nanowires of high crystalline quality is attractive for the initial exploration of new materials. These tube furnaces eliminated the necessity for sophisticated reactors nominally used in metalorganic chemical vapor deposition or molecular beam epitaxy.

The development of nanowire lasers made from GaN also represents the first extension of the single nanowire laser to new material systems beyond ZnO.[30] Single-crystalline GaN nanowires were grown in a bottom up synthesis for single nanowire lasers. A year later, the first example of lasing from a core-shell heterostructure was demonstrated, which consisted of a GaN core with an epitaxial shell of $Al_{0.75}Ga_{0.25}N$.[31] The core-shell nanowires were synthesized by a one-step CVD process with spontaneous phase separation within the synthesized nanowires forming a 5 to 40 nm thick GaN core. The $Al_{0.75}Ga_{0.25}N$ shell forms a type-I junction with GaN and possesses a smaller refractive index than the GaN (2.54 and 2.25, respectively), which enables this structure to function as a thin GaN quantum wire core embedded in AlGaN cladding. Overall, these works opened up the way for the study of new material systems and

heterostructures for nanowire lasers as described in the remainder of this review. Since these early works, the library of nanowire laser materials has expanded enormously, resulting in nano-lasers that emit in the UV, the visible, and the near-IR. This wide range in emission wavelengths can be seen in demonstrations for ZnO,[15,18,30] GaN,[17,26] InGaN,[32] CdS,[33] CdSe,[34] CdSSe,[35] GaAs,[36] InGaAs,[37] AlGaAs,[38] ZnS,[39] CdSe,[34] GaSb,[40] and InP.[41,42]

New Nanowire Laser Cavity Structures

The compact form-factor of one-dimensional nanowire lasers has also enabled the development of nanowires for photonic applications such as nanoscale optical routing,[43] nanoscale electro-optic modulators,[44] and single-cell probes.[45] A range of alternative cavity structures have also been explored through either bottom-up or top-down fabrication strategies. One of the first alternative structures was an adaptation of the vertical ZnO array; by carefully controlling the nanowire growth conditions,[46] dendritic ZnO nanowires could be grown from a ZnO backbone.[47] The ZnO nanowires within these linear, regularly spaced arrays exhibited amplified spontaneous emission at elevated pumping thresholds, which was similar to the previously reported planar arrays and were hypothesized to form modified Fabry-Pérot cavities with only a single, well-defined end facet.

Physical manipulation of flexible nanowires provides a method for generating cavities of arbitrary geometry with improved performance. One example is the ring resonator nanowire laser. Ring resonators are typically formed by bending a pre-existing nanowire into a continuous loop. If the overlapping nanowire sections are sufficiently coupled to allow for recirculation of light around the loop, optical feedback is increased within the system, thereby lowering the lasing threshold. The first example of a nanowire ring resonator was made from GaN and manipulated into a loop with the two ends side-by-side.[48] Cavity modes were observed in the spontaneous emission and lasing spectra indicating the formation of a circular resonator. In this case, when the nanowire ring resonator cavities were decoupled into linear cavities, the Q-factor of the resonator was shown to drop 40%, which showed that the ring resonators have larger Q-factors than their linear counterparts. The ring resonator cavity has been improved substantially over the years, but mechanical instability has been a significant issue that has limited the application of these cavities. A recent report improved the mechanical stability of the ring resonator by splicing the ends together using a short poly(styrene) nanowire segment.[49] While

the splice increased the lasing threshold slightly, the enhanced mechanical stability should allow for a wider range of applications including their use in liquid media.

Alternative cavity geometries have also been explored to improve nanowire laser performance. For instance, to achieve single-mode lasing in single nanowires, there is generally a tradeoff between engineering a single mode laser without sacrificing material gain, which can result in an increased lasing threshold.[50] An alternative strategy relies on the formation of a cleaved-coupled cavity.[26] By cleaving a nanowire in two at a determined point, all but a single lasing mode may be suppressed. This demonstration shows that adding additional gain to a single nanowire in a specified geometry can reduce the lasing threshold and control the lasing modes to improve emission quality. The technique relies on calculations of both the gap position and the size of each cavity to modulate the lasing threshold of all the longitudinal modes. This process was recently shown for a GaN nanowire cleaved using focused ion beam milling (Figure 4).
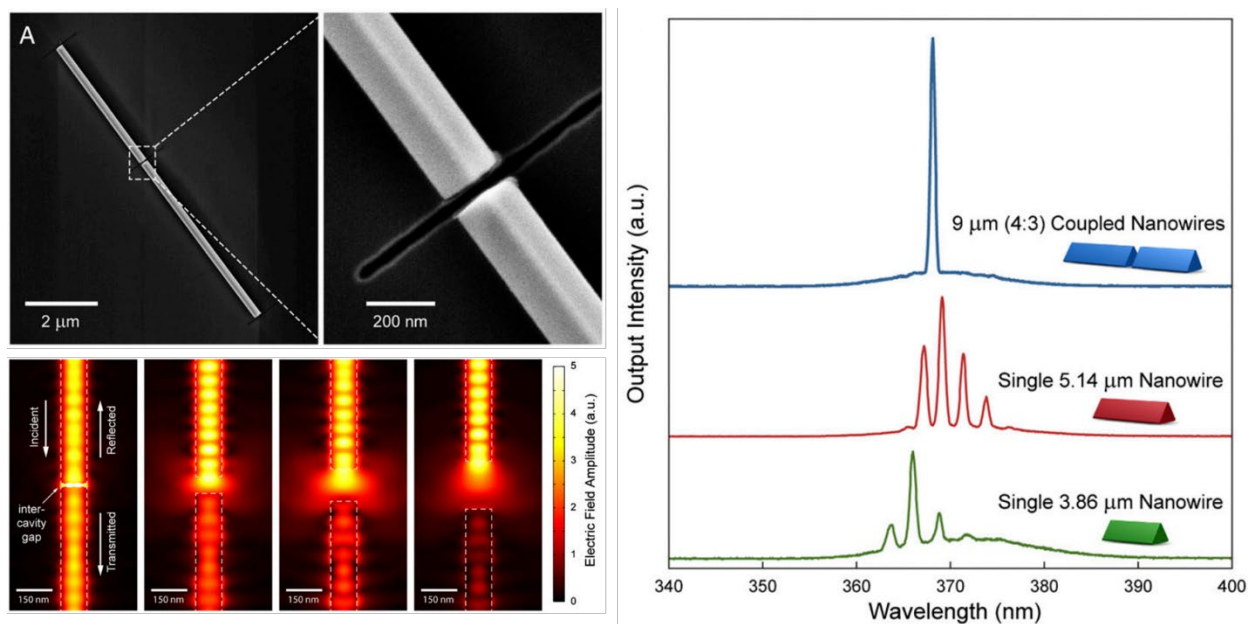

Figure 4. A) Scanning electron micrograph of a GaN cleave coupled nanowire laser cavity. The gap size and position were chosen to optimize the cavity for single mode lasing. B) Finite element method simulations depicting the transmission and reflectance of a waveguide mode as a function of gap size. C) Photoluminescence spectra depicting the lasing modes of the individual nanowire components (red and green) and the coupled nanowires (blue). Adapted with permission from ref 26.

Additionally, there have been a number of reports of assembling nanowires into hierarchical photonic structures or integrating them into microresonator structures to form hybrid photonic devices for exploring cutting-edge optical phenomena. These devices rely on supporting structures that are optically coupled to a nanowire that provides gain. The first study involved coupling a CdS nanowire to a resonator microcavity.[51] The microcavity design was guided by finite-difference time-domain (FDTD) simulation to demonstrate that lasing was possible in both linear as well as racetrack-style microcavities. A recently reported, alternative process utilized bottom-up synthesis exclusively to grow a photonic crystal comprised of a well-ordered nanowire array.[52] Each nanowire was made up of a GaAs/InGaAs/GaAs axial heterostructure, with the central InGaAs section acting as the gain medium. These advances in incorporating nanowires into hierarchical or other photonic structures showcase the flexibility of a nanowire for integration with photonic structures. Taking these integration concepts a step further, Das and coworkers used a GaN nanowire to reduce the threshold of a room temperature polariton laser.[53] The researchers accomplished this feat by integrating a GaN nanowire grown inside a microcavity with the nanowire growth direction perpendicular to the optical axis of the cavity. This strategy enabled them to circumvent the internal polarization field of GaN, which likely lowered the quantum efficiency in previous GaN-based microcavity lasers via the quantum-confined Stark effect.[54] These studies highlight how nanowires can be used with conventional photonic structures to explore optical phenomena and demonstrate devices with excellent optical performance.

Wavelength Tunable Nanowire Lasers

Many photonics applications could be enabled or enhanced by the use of wavelength tunable, nanoscale lasers such as sensing,[55] white light generation,[56,57] and optoelectronic integrated circuits.[13] Discrete color tunability can be achieved by using different gain materials, with the ultimate goal of achieving continuous wavelength tunability to tailor emission to a specific application. Another approach to tune the wavelength is by modifying the dielectric environment of the cavity via excitation intensity,[30] cavity length,[58] substrate,[59] or cavity design.[48,60] However, this strategy can only be applied over limited wavelength ranges and can be impractical to implement in some cases. Here, we focus our discussion on tuning the composition for controlling the emission wavelength.

Alloying of semiconductors is a well-known technique for modifying the band gap of a material and has been applied to a variety of semiconductors to achieve continuous alloying.[61] In some materials, phase separation issues have arisen in alloyed thin films due to lattice mismatch. Many of these problems have been overcome in nanowires by carefully controlling the growth conditions. Compositional tunability within CdS_xSe_{1-x} nanowires on the same chip was demonstrated by Ning and coworkers.[35] Through careful control of the temperature gradient within the growth furnace, CdS_xSe_{1-x} nanowires were grown with x = 0 to 1 over a relatively short 1.2 cm substrate. These nanowire arrays exhibited chip position-dependent emission ranging from 498 nm to 692 nm, and upon optical excitation above the lasing threshold, the nanowires were found to lase across an unprecedented 189 nm wavelength range. Extending this technique further, the growth of compositionally variable nanoribbons of CdS_xSe_{1-x}, as well as $Zn_\gamma Cd_{1-\gamma}S$ was also demonstrated.[62] These nanoribbons were found to lase from the UV (340 nm) to the near-IR (710 nm), with well-defined growth parameters providing precise control over the emission wavelength to achieve overlapping coverage across the spectrum. Besides these proven nanowire lasers, other strategies have been developed over the years to grow promising, compositionally-graded nanowires. For instance, in addition to temperature gradient control, a gradient of source material composition was also exploited to grow $In_xGa_{1-x}N$ alloy,[63] where the full composition range between InN and GaN was realized for the first time. The demonstration of alloy composition control through temperature gradient[35] and elemental gradient[63] lead naturally to the simultaneous exploration of both gradients using a growth apparatus which provided substrate tilting and optimization of temperature profile.[64,65] This dual gradient method led to the growth of $Zn_xCd_{1-x}S_ySe_{1-y}$ in its full composition range from ZnS to CdSe on a single substrate with emission in the full visible spectrum.[65] With further development, these methods for synthesizing broadly tunable materials may provide more facile assess to high quality nanowires for lasing.

This concept of compositional control providing emission tunability has also been demonstrated within compositionally graded single nanowires of CdS_xSe_{1-x}.[66] Due to asymmetric light propagation, a compositionally graded nanowire will lase only at the lowest energy wavelength as all higher energy emission is attenuated by the low band gap portions of the nanowire.[67] However, by folding the wide band gap side of the flexible nanowires into a loop cavity, simultaneous lasing could be observed at different wavelengths within the same

nanowire.[68] Tunability over the red-green portion of the spectrum was achieved through variable optical pumping, such that the output ratio from the two cavities could be tuned continuously between the two colors. By incorporating a third, blue loop cavity, this approach may allow for continuous tunability across the entire visible spectrum. The most recent strategy for controlling the lasing wavelength of compositionally-graded CdS_xSe_{1-x} nanowires relies on cleaving the nanowires to the proper size (Figure 5a).[69] The lasing wavelength may be selected by using a bend-to-facture method on the nanowire to remove undesired low band gap material. The free spectral range, or the mode spacing dictated by the length of the Fabry-Perot cavity, may be tuned by removing material from the high band gap end without significantly changing the lasing wavelength. These two operations can provide highly tunable, single mode nanowire lasers. This approach was demonstrated by Yang and coworkers who showed that the CdS_xSe_{1-x} nanowires may be predictably sized to yield nanowire lasers operating over a wide spectral range (119 nm).

Recently, methyl ammonium lead halide perovskites were identified as a promising gain material with potential for application in a variety of optoelectronic systems.[70,71] These inorganic-organic hybrid materials exhibit high absorption cross sections, efficient photoluminescence, long diffusion lengths, and low trap state densities.[70] Initial reports of amplified spontaneous emission (ASE) in hybrid perovskite thin films indicated that methyl ammonium lead iodide ($MAPbI_3$) exhibited high material gain with a low ASE threshold.[72] In addition, by using a mixture of methyl ammonium salts in the film fabrication, wide wavelength tunability of the ASE peak was demonstrated. This study was followed rapidly by detailed photophysical studies, which reported that a bimolecular free carrier electron−hole recombination mechanism was responsible for the 70% photoluminescence quantum efficiency observed in thin films of $MAPbI_3$.[73] Besides ASE from thin films,[74] low threshold lasing in $MAPbI_3$ films contained in a vertical cavity optical structure was also demonstrated. These initial reports established the ease with which perovskite materials could be made to lase while also providing the foundation for other laser cavity designs. The first report of lasing in a nanowire cavity was recently reported by Zhu and coworkers, where the critical breakthrough was the synthesis of nanowires with high optical quality and suitable dimensions.[75] The nanowires were grown by exposing a lead acetate film to a solution of methyl ammonium halide salt. These nanowires were shown to lase at room temperature under optical excitation. Furthermore, the authors were able to tune the composition of the nanowires by changing the ratio of halide salts

in the growth solution to yield lasing across the visible spectrum (Figure 5b). While these nanowires were remarkable, what is even more impressive is the fact that they were grown under ambient conditions. This is in stark contrast to most other nanowire lasers, which rely on high temperatures or vacuum processes to produce suitable nanowires. Notably, another approach was tried by Xing and coworkers where PbI_2 nanowires were first grown, followed by exposure to methyl ammonium halide vapor for the final conversion to the perovskite nanowire.[76] While the nanowire morphology was maintained, the lasing properties were significantly less impressive than those achieved with the solution-phase growth method, suggesting the solution phase method produced superior quality nanowire lasers.

While exhibiting excellent performance, hybrid perovskite nanowires are well known for their intrinsic instability.[77,78] A variety of strategies have been pursued to improve stability, many focusing on removing the reactive methyl ammonium cation and replacing it with an inorganic or aprotic cation. In particular, cation replacement with cesium has opened up a new route to highly luminescent, stable materials.[79] The first reports of colloidal nanocrystals made from cesium lead halides demonstrated similar wavelength tunability much in the same way as the hybrids perovskite materials with remarkably high photoluminescence quantum efficiencies.[80,81] As with hybrid perovskite materials, ASE was demonstrated in thin films of nanocrystals with a similarly low lasing threshold.[82,83] These reports were followed quickly by the synthesis and characterization of colloidal[84] and non-colloidal[85] cesium lead halide perovskite nanowires. The non-colloidal, $CsPbBr_3$ nanowires were found to have comparable lasing thresholds and Q-factors to the hybrid perovskite nanowire lasers with a significant different: they were found to be ultra-stable under lasing conditions, lasting for over 10^9 excitation cycles.[85] High stability was also observed for lasing under ambient conditions as well as during storage under ambient conditions. Easily attainable growth conditions, high performance characteristics, and improving stability make perovskite-based nanowire lasers a promising material for the future.
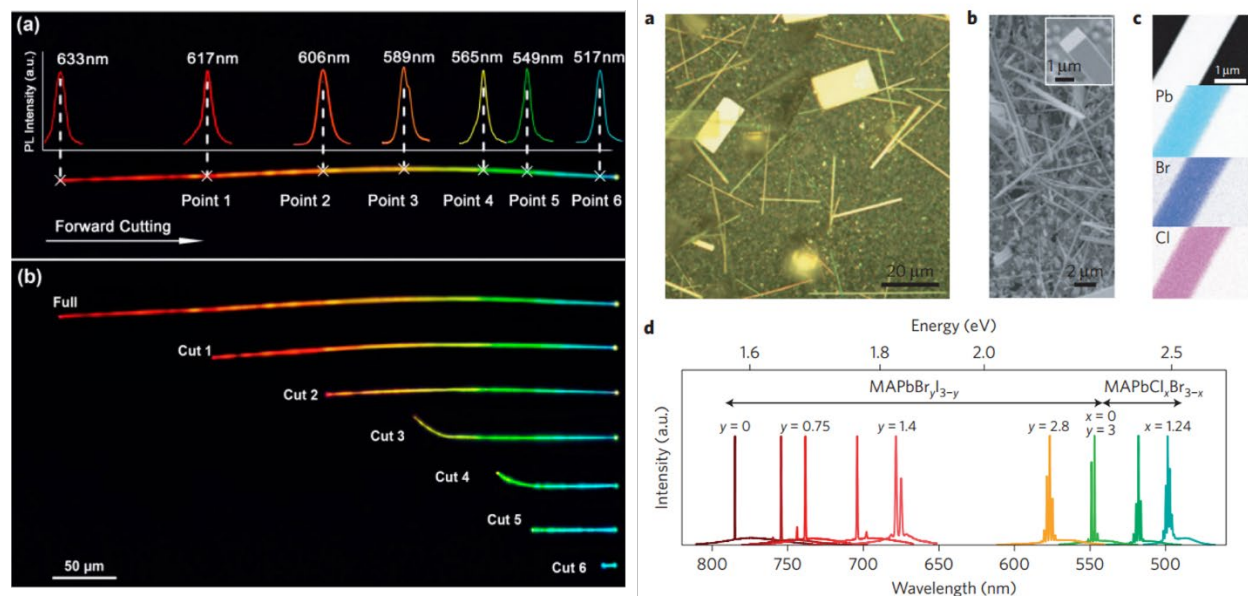
Figure 5. A) Compositionally graded CdS_xSe_{1-x} nanowire photoluminescence spectra and B) optical images under laser excitation demonstrating nanowire position-dependent emission. Adapted from ref 69. C) Optical and D) SEM images of alloyed methylammonium lead halide nanowires and plates. E) SEM image (top) and EDS images depicting the elemental distribution of Pb, Br, and Cl within the alloyed nanowire. F) Broad wavelength tunability achieved over nearly 300 nm by tuning the elemental composition of the nanowire laser. Adapted from ref 75.

Surface Plasmon Polariton Nanowire Lasers

Laser miniaturization via the semiconductor nanowire is limited by the diameter of the nanowire to approximately half the optical wavelength, which is known as the diffraction limit. However, nanowires can be used as platforms for creating a new type of laser based on surface plasmon polaritons (SPP).[86,87] SPP waves, which are the collective oscillations of electrons on the surface of a metal, have significantly shorter wavelengths than the photonic wavelengths of the same energy, which allows the laser cavity to store and guide optical energy far below the optical diffraction limit. The main challenge in creating a plasmonic laser has been to overcome the intrinsic absorption losses of the metal,[88] which prevents optical energy from amplifying within a cavity. The strategy of applying a silver coating to a nanowire laser in order to harness SPP for lasing and reduce the overall size of the laser structure was first studied theoretically in 2007.[89] These studies suggested the existence of wavelength regions where the nanowire optical gain could exceed the metal loss to achieve an overall positive gain. To further minimize these

losses, a new type of cavity was created by placing a dielectric spacer in between the metal and the gain medium to create a hybrid plasmonic cavity.[90,91] This strategy allows for most of the optical energy to be contained within the spacer rather than the metal, thereby reducing metal loss.

The initial theoretical work predicted a dielectric/metal hybrid structure could be a successful platform for lasing.[91] This was followed by the first report of SPP nanowire lasing in a horizontal CdS nanowire on a silver substrate separated by a nanoscale film of MgF_2, which provides control over optical confinement, insulates the wire from the metal, and provides a transverse hybrid cavity (Figure 6).[92] Through optical pumping, characteristic signatures of lasing were observed and indicated that the plasmonic nanowires were operating in a Fabry-Pérot geometry. Besides plasmonic lasing, photonic lasing was easily achieved by exchanging the silver substrate with quartz, which allowed for a direct performance comparison. While both types exhibited similar thresholds due to similar cavity structure, there was a significant difference in diameter dependence. With decreasing nanowire diameter, photonic lasing ceased near 150 nm as optical confinement broke down. However, plasmonic lasing persisted down to 52 nm. Furthermore, measurements of the polarization of the emission confirmed the existence of plasmonic modes because plasmons are strictly longitudinal, while photonic modes have significant transverse polarization. In addition, similar research based on GaN nanowires on single crystal silver[93] and ZnO nanowires[94] for operation near the SPP resonance has continued in the last few years, leading to new interesting results for low threshold[93] and ultrafast operation.[94]

One of the drawbacks of a transverse hybrid cavity is the inability to separate contributions from the plasmonic and photonic components of the cavity. Recently, a unique cavity scheme was devised to address this issue: a curved CdSe nanowire was brought into contact with the side of a curved silver nanowire so that they coupled at a small point.[95] This arrangement provided a longitudinal hybrid cavity such that optical excitation of the CdSe nanowire and subsequent wave guiding generated SPP waves in the silver nanowire. The geometry provided spatial separation between simultaneous plasmonic and photonic contributions to the emission output. Upon excitation of the CdSe portion of the cavity, light output was observed from the silver nanowire end of the cavity indicating efficient photon-to-plasmon coupling. By measuring the emission output from the silver nanowire, the authors were

able to observe a strong polarization-dependence indicative of the electromagnetic nature of the SPP waves. An interesting feature of this demonstration is that a strongly localized, coherent, SPP source could be "delivered" to another point. While great challenges still exist in minimizing metal losses and improving overall gain efficiency, SPP nanowire lasers offer significant advantages such as improved thermal management.
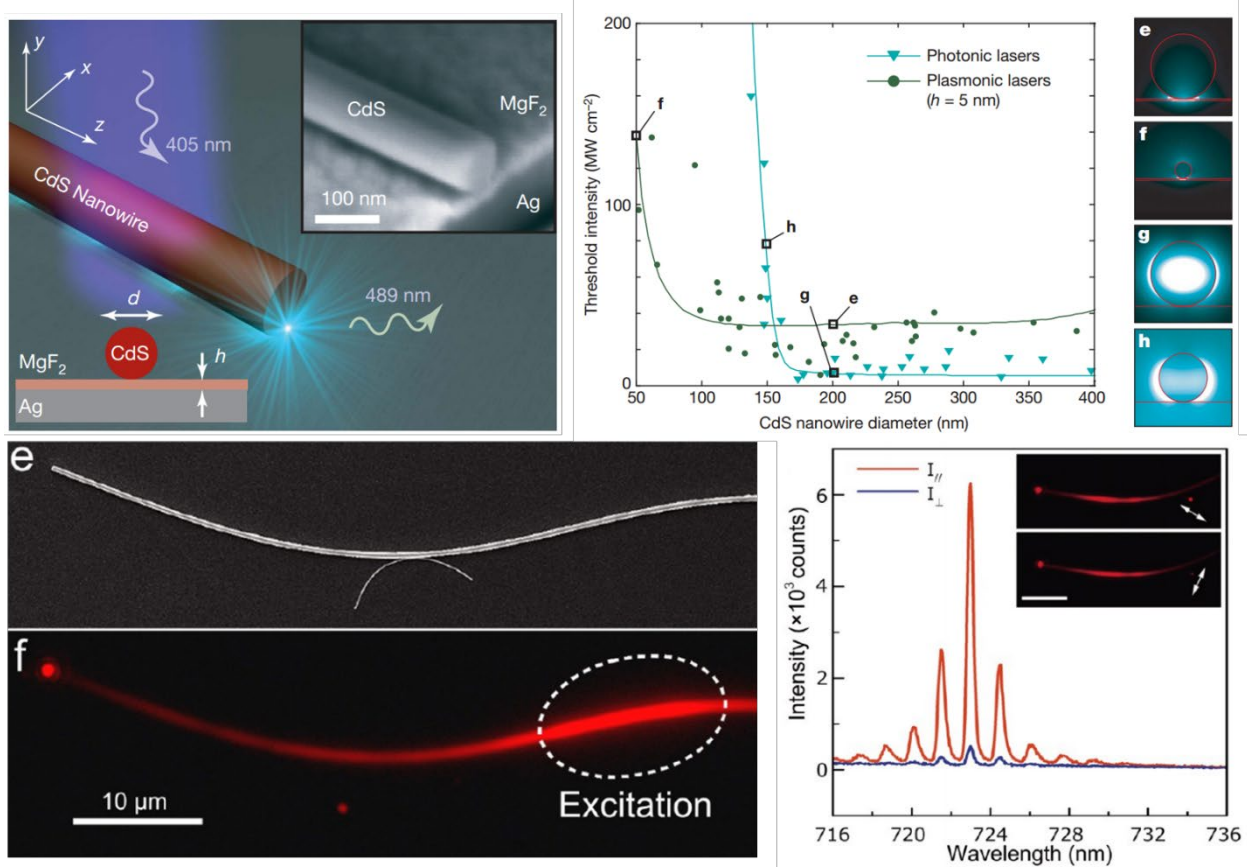

Figure 6. Top row – A) Depiction of a CdS nanowire on a silver substrate forming a SSP laser cavity under optical excitation. B) Lasing threshold intensity as a function of nanowire diameter for photonic (blue triangles) and plasmoinc laser cavities. SSP nanowire cavities are able to lase with significantly smaller diameters than photonic cavities indicating the plasmonic nature of the cavity. C-F) Simulations of guided modes for plasmonic (C,D) and photonic (E,F) nanowire laser cavities. Adapted with permissions from ref 92. Bottom row – A) Scanning electron micrograph and B) optic image of CdSe nanowire coupled to a silver nanowire. C) Excitation of the CdSe nanowire results in polarization dependent emission from the silver nanowire end-facet. Adapted with permissions from ref 95.

Electrical Excitation of Nanowire Lasers

The nanowire lasers discussed thus far have been excited optically by another laser orders of magnitude larger. While suitable for the fundamental study and development of new gain media and cavity architectures, optical excitation is unsuitable for most of the intended nanowire laser applications, especially in the area of on-chip integrated photonics. Therefore, carrier excitation via electrically pumping is a much more desirable approach. The ultimate goal for semiconductor nanowire lasing hinges on achieving reliable lasing through electrical injection of electrons and holes into a metal-dielectric composite nanowire structure. The principal challenge in realizing electrically pumped nanowire lasers is to integrate electrodes without diminishing the quality of the cavity to the point where lasing is no longer possible. As with plasmonic lasers, metal-loss, the process where optical energy is absorbed and dissipated via electron scattering and thermalization in a metal, has been identified as the primary loss mechanism in electrically pumped cavities.[88] Overcoming this has been a high priority and has been pursued through a number of different approaches.

Lithographic, top-down techniques are currently the most viable approach for electrically driven nanowire lasers. The first report of electrically pumped nanowire lasing used a horizontal CdS nanowire on a p^{++}-Si substrate, which was then coated with an insulating layer of Al_2O_3 followed by a Ti/Au injection layer.[96] Almost a decade would pass before another promising device architecture arose in the semiconductor core-metal shell[89] structure realized by Hill and coworkers[97] using a top-down fabrication process. Extensive modeling and experimental work by Hill, Ning, and their coworkers demonstrated that a semiconductor-metal core-shell structure can facilitate gain for lasing and is amenable for electrical injection.[89,97,98] As a demonstration of electrical injection lasing, a n-InP/InGaAs/p-InP micropillar was etched from a metalorganic chemical vapor deposition-grown wafer to provide the gain medium and optical cavity, while current injection was provided by a p-InGaAsP substrate and a Ag/SiN conductor/insulator layer (Figure 7).[99] Initial devices demonstrated light emission characteristic of lasing, but the performance was inhibited by significant heating. This barrier was recently overcome through improving the structure and thermal management of the device.[98,100] The newest generation of devices showed lasing thresholds of 1.2 mA under DC bias and operation at over twice the threshold current. This remarkable work is the first well-understood demonstration of lasing in a near-nano sized cavity. A recent report built upon this initial demonstration by showing that

control over the lasing wavelength as well as emission polarization was possible.[101] A similar, cylindrical cavity was electrically pumped and found to output azimuthally polarized light, which is critical for particle trapping and high resolution imaging. Facile lasing wavelength control from 1.37 μm to 1.53 μm was achieved by adjusting the cavity diameter during device fabrication.

Another strategy for electrical pumping relies on nanowire arrays grown directly on conducting substrates followed by post-synthetic introduction of the second contact. Recent studies have reported electrically pumped random lasing in AlGaN nanowire arrays.[102] By utilizing the Anderson localization of light in AlGaN/GaN heterostructures, random lasing in the UV spectral region was reported in a lithography-free nanowire array. The nanowire array was grown using molecular beam epitaxy to form an AlGaN active layer sandwiched between two p- and n- doped AlGaN cladding layers, with the structures templated from Si-doped GaN on n-Si. Successful CW operation was observed from 6 – 100 K with a lasing threshold of 12 A cm^{-2} and operational stability at over six times the threshold current. Emission wavelength tunability from 319 – 335 nm was also observed for various regions depending on the nature of the gain cavity. Further wavelength tunability was achieved afterward by utilizing quantum confinement.[103] The AlGaN gain medium was fabricated as a collection of nanoparticles which lased at 262.1 nm with comparable lasing thresholds at 77 K. These reports show some potentially promising directions for developing better electrically injected nanowire lasers.
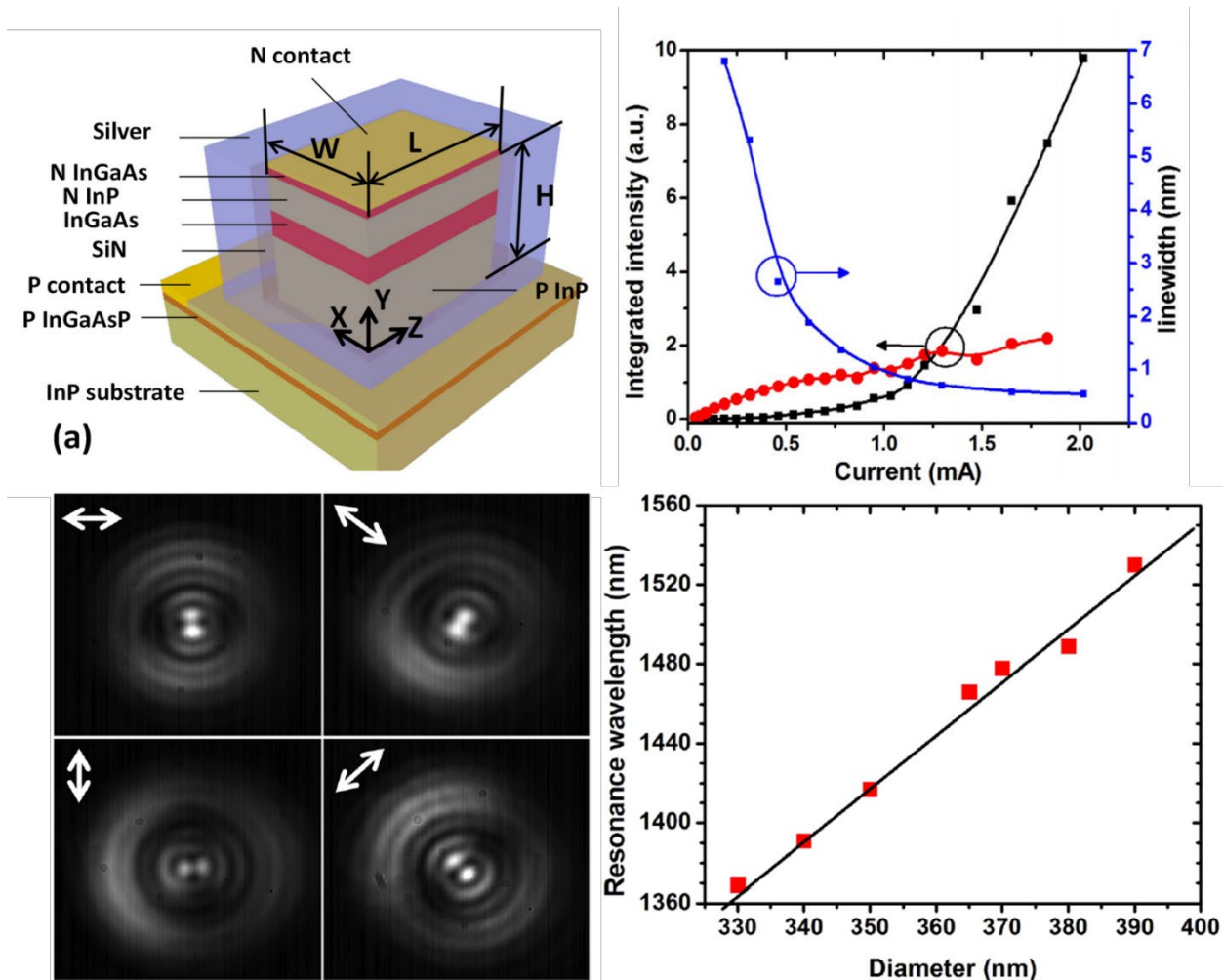
Figure 7. A) A cross-sectional diagram of an InGaAs/InP metallic laser cavity. B) Integrated emission intensity and linewidth (blue) as a function of device current showing a superliner increase of emission with decreasing linewidth. Adapted with permissions from ref 100. C) Four polarized emission images (polarizer direction given by white arrow) from a cylindrical, electrically pumped cavity demonstrating azimuthal emission polarization. D) The linear dependence between nanowire cavity diameter and laser emission wavelength. Adapted with permissions from ref 101.

Conclusions

Research conducted over the last fifteen years has significantly advanced the field of semiconductor nanowire lasers. Progress in a range of frontiers has been achieved including an expanded range of materials, greater alloy composition control, varied cavity structures, improved mode control, and reduced lasing thresholds. Development of wavelength tunable,

solution processable perovskite nanowire lasers has established a promising class of materials capable of record-breaking performance. Improvement of design, performance, and overall understanding of plasmonic nanowire lasers opens up promising avenues for the development of ultra-small laser cavities. While impressive progress has been made including room temperature operation which was thought impossible initially, novel design and reduction of metal loss are still crucial for further improving the device performance. Finally, with more progress in the development of electrically pumped nanoscale lasers, future integration of these devices into optoelectronic circuits is within reach. Ultimately, semiconducting nanowire lasers are incredibly versatile nanoscale light sources. While they range widely in terms of their composition, geometry, cavity structure, and lasing mechanism, all have the potential to supply light for integrated photonics applications. By expanding the capabilities and improving performance of semiconducting nanowire lasers, the scientific community will surely discover new insights and applications to advance the field.

REFERENCES

1   Einstein, A. Strahlungs-emission und absorption nach der quantentheorie. *Deutsche Physikalische Gesellschaft* **18**, 318-323, (1916).

2   Schawlow, A. L. & Townes, C. H. Infrared and optical masers. *Phys. Rev.* **112**, 1940-1949, (1958).

3   Maiman, T. H. Stimulated optical radiation in ruby. *Nature* **187**, 493-494, (1960).

4   Rosenberg, N. & Trajtenberg, M. A general purpose technology at work: The Corliss steam engine in the late 19th century US. *National Bureau of Economic Research Working Paper Series* **No. 8485**, (2001).

5   Council, N. R. *Optics and photonics: Essential technologies for our nation*. (The National Academies Press, 2013).

6   Agrawal, G. P. & Dutta, N. K. *Infrared and visible semiconductor lasers*. (Springer, 1993).

7   Choquette, K. D. & Hou, H. Q. Vertical-cavity surface emitting lasers: Moving from research to manufacturing. *Proc. IEEE* **85**, 1730-1739, (1997).

8   Mahler, L. *et al.* Vertically emitting microdisk lasers. *Nature Photon.* **3**, 46-49, (2009).

9   Altug, H. & Vučković, J. Photonic crystal nanocavity array laser. *Opt. Express* **13**, 8819-8828, (2005).

10   Ning, C. Z. in *Advances in semiconductor lasers* (eds James J. Coleman, A. Catrina Bryce, & Chennupati Jagadish) 455-486 (Academic Press, 2012).

11   Ma, R.-M., Ota, S., Li, Y., Yang, S. & Zhang, X. Explosives detection in a lasing plasmon nanocavity. *Nature Nanotechnol.* **9**, 600-604, (2014).

12   Ma, Y., Guo, X., Wu, X., Dai, L. & Tong, L. Semiconductor nanowire lasers. *Adv. Opt. Photonics* **5**, 216-273, (2013).

13   Yan, R., Gargas, D. & Yang, P. Nanowire photonics. *Nature Photon.* **3**, 569-576, (2009).

14   Wagner, R. S. & Ellis, W. C. Vapor-liquid-solid mechanism of single crystal growth. *Appl. Phys. Lett.* **4**, 89-90, (1964).

15   Huang, M. H. *et al.* Room-temperature ultraviolet nanowire nanolasers. *Science* **292**, 1897-1899, (2001).

16   Huang, M. H. *et al.* Catalytic growth of zinc oxide nanowires by vapor transport. *Adv. Mater.* **13**, 113-116, (2001).

17   Johnson, J. C. *et al.* Single gallium nitride nanowire lasers. *Nature Mater.* **1**, 106-110, (2002).

18   Johnson, J. C. *et al.* Single nanowire lasers. *J. Phys. Chem. B* **105**, 11387-11390, (2001).

19   Maslov, A. V. & Ning, C. Z. Far-field emission of a semiconductor nanowire laser. *Opt. Lett.* **29**, 572-574, (2004).

20   Coldren, L. A. & Corzine, S. W. *Diode lasers and photonic integrated circuits*. (John Wiley & Sons Inc., 1995).

21   Siegman, A. E. *Lasers*. (University Science Books, 1986).

22   Maslov, A. V. & Ning, C. Z. Reflection of guided modes in a semiconductor nanowire laser. *Appl. Phys. Lett.* **83**, 1237-1239, (2003).

23   Maslov, A. V. & Ning, C. Z. Modal gain in a semiconductor nanowire laser with anisotropic bandstructure. *Quantum Electronics, IEEE Journal of* **40**, 1389-1397, (2004).

24   Ning, C. Z. *et al.* in *Photonics Society Summer Topical Meeting Series, 2014 IEEE.* 23-24.

25   Ning, C. Z. What is laser threshold. *Selected Topics in Quantum Electronics, IEEE Journal of* **19**, 1503604-1503604, (2013).

26   Gao, H., Fu, A., Andrews, S. C. & Yang, P. Cleaved-coupled nanowire lasers. *Proc. Natl. Acad. Sci. U. S. A.* **110**, 865-869, (2013).

27   Björk, G., Karlsson, A. & Yamamoto, Y. Definition of a laser threshold. *Physical Review A* **50**, 1675-1680, (1994).

28   Zimmler, M. A., Bao, J., Capasso, F., Müller, S. & Ronning, C. Laser action in nanowires: Observation of the transition from amplified spontaneous emission to laser oscillation. *Appl. Phys. Lett.* **93**, 051101, (2008).

29   Chow, W. W., Jahnke, F. & Gies, C. Emission properties of nanolasers during the transition to lasing. *Light Sci. Appl.* **3**, e201, (2014).

30   Johnson, J. C., Yan, H., Yang, P. & Saykally, R. J. Optical cavity effects in ZnO nanowire lasers and waveguides. *J. Phys. Chem. B* **107**, 8816-8828, (2003).

31   Choi, H.-J. *et al.* Self-organized GaN quantum wire UV lasers. *J. Phys. Chem. B* **107**, 8721-8725, (2003).

32   Qian, F. *et al.* Multi-quantum-well nanowire heterostructures for wavelength-controlled lasers. *Nature Mater.* **7**, 701-706, (2008).

33   Agarwal, R., Barrelet, C. J. & Lieber, C. M. Lasing in single cadmium sulfide nanowire optical cavities. *Nano Lett.* **5**, 917-920, (2005).

34   Pan, A. *et al.* Fabrication and red-color lasing of individual highly uniform single-crystal CdSe nanobelts. *J. Phys. Chem. C* **111**, 14253-14256, (2007).

35   Pan, A. *et al.* Continuous alloy-composition spatial grading and superbroad wavelength-tunable nanowire lasers on a single chip. *Nano Lett.* **9**, 784-788, (2009).

36   Saxena, D. *et al.* Optically pumped room-temperature gaas nanowire lasers. *Nature Photon.* **7**, 963-968, (2013).

37   Chen, R. *et al.* Nanolasers grown on silicon. *Nature Photon.* **5**, 170-175, (2011).

38 Mayer, B. *et al.* Lasing from individual GaAs-AlGaAs core-shell nanowires up to room temperature. *Nature Comm.* **4**, (2013).

39 Zapien, J. A. *et al.* Room-temperature single nanoribbon lasers. *Appl. Phys. Lett.* **84**, 1189-1191, (2004).

40 Chin, A. H. *et al.* Near-infrared semiconductor subwavelength-wire lasers. *Appl. Phys. Lett.* **88**, 163115, (2006).

41 Gao, Q. *et al.* Selective-area epitaxy of pure wurtzite InP nanowires: High quantum efficiency and room-temperature lasing. *Nano Lett.* **14**, 5206-5211, (2014).

42 Zhang, L. *et al.* Wide InP nanowires with wurtzite/zincblende superlattice segments are type-II whereas narrower nanowires become type-I: An atomistic pseudopotential calculation. *Nano Lett.* **10**, 4055-4060, (2010).

43 Sirbuly, D. J. *et al.* Optical routing and sensing with nanowire assemblies. *Proc. Natl. Acad. Sci. U. S. A.* **102**, 7800-7805, (2005).

44 Greytak, A. B., Barrelet, C. J., Li, Y. & Lieber, C. M. Semiconductor nanowire laser and nanowire waveguide electro-optic modulators. *Appl. Phys. Lett.* **87**, 151103, (2005).

45 Shambat, G. *et al.* Single-cell photonic nanocavity probes. *Nano Lett.* **13**, 4999-5005, (2013).

46 Yang, P. *et al.* Controlled growth of ZnO nanowires and their optical properties. *Adv. Funct. Mater.* **12**, 323-331, (2002).

47 Yan, H. *et al.* Dendritic nanowire ultraviolet laser array. *J. Am. Chem. Soc.* **125**, 4728-4729, (2003).

48 Pauzauskie, P. J., Sirbuly, D. J. & Yang, P. Semiconductor nanowire ring resonator laser. *Phys. Rev. Lett.* **96**, 143903, (2006).

49 Hu, Z., Guo, X. & Tong, L. Freestanding nanowire ring laser. *Appl. Phys. Lett.* **103**, 183104, (2013).

50 Li, Q. *et al.* Single-mode GaN nanowire lasers. *Opt. Express* **20**, 17873-17879, (2012).

51 Barrelet, C. J. *et al.* Hybrid single-nanowire photonic crystal and microresonator structures. *Nano Lett.* **6**, 11-15, (2006).

52 Scofield, A. C. *et al.* Bottom-up photonic crystal lasers. *Nano Lett.* **11**, 5387-5390, (2011).

53 Das, A. *et al.* Room temperature ultralow threshold GaN nanowire polariton laser. *Phys. Rev. Lett.* **107**, 066405, (2011).

54 Hisashi, M. *et al.* Quantum-confined stark effect on photoluminescence and electroluminescence characteristics of InGaN-based light-emitting diodes. *J. Phys. D: Appl. Phys.* **41**, 165105, (2008).

55 Kotani, A. *et al.* Endov/DNA ligase mutation scanning assay using microchip capillary electrophoresis and dual-color laser-induced fluorescence detection. *Anal. Methods* **4**, 58-64, (2012).

56 Neumann, A. *et al.* Four-color laser white illuminant demonstrating high color-rendering quality. *Opt. Express* **19**, A982-A990, (2011).

57 Fan, F., Turkdogan, S., Liu, Z., Shelhammer, D. & Ning, C. Z. A monolithic white laser. *Nature Nanotechnol.* **10**, 796-803, (2015).

58 Li, J. *et al.* Wavelength tunable CdSe nanowire lasers based on the absorption-emission-absorption process. *Adv. Mater.* **25**, 833-837, (2013).

59   Liu, X., Zhang, Q., Yip, J. N., Xiong, Q. & Sum, T. C. Wavelength tunable single nanowire lasers based on surface plasmon polariton enhanced Burstein–Moss effect. *Nano Lett.* **13**, 5336-5343, (2013).

60   Xiao, Y., Meng, C., Wu, X. & Tong, L. Single mode lasing in coupled nanowires. *Appl. Phys. Lett.* **99**, 023109, (2011).

61   Zhuang, X., Ning, C. Z. & Pan, A. Composition and bandgap-graded semiconductor alloy nanowires. *Adv. Mater.* **24**, 13-33, (2012).

62   Zapien, J. A. *et al.* Continuous near-infrared-to-ultraviolet lasing from II-VI nanoribbons. *Appl. Phys. Lett.* **90**, 213114, (2007).

63   Kuykendall, T., Ulrich, P., Aloni, S. & Yang, P. Complete composition tunability of InGaN nanowires using a combinatorial approach. *Nature Mater.* **6**, 951-956, (2007).

64   Pan, A., Liu, R., Sun, M. & Ning, C.-Z. Quaternary alloy semiconductor nanobelts with bandgap spanning the entire visible spectrum. *J. Am. Chem. Soc.* **131**, 9502-9503, (2009).

65   Pan, A., Liu, R., Sun, M. & Ning, C.-Z. Spatial composition grading of quaternary ZnCdSSe alloy nanowires with tunable light emission between 350 and 710 nm on a single substrate. *ACS Nano* **4**, 671-680, (2010).

66   Gu, F. *et al.* Spatial bandgap engineering along single alloy nanowires. *J. Am. Chem. Soc.* **133**, 2037-2039, (2011).

67   Xu, J. *et al.* Asymmetric light propagation in composition-graded semiconductor nanowires. *Sci. Rep.* **2**, 820, (2012).

68   Liu, Z. *et al.* Dynamical color-controllable lasing with extremely wide tuning range from red to green in a single alloy nanowire using nanoscale manipulation. *Nano Lett.* **13**, 4945-4950, (2013).

69   Yang, Z. *et al.* Broadly defining lasing wavelengths in single bandgap-graded semiconductor nanowires. *Nano Lett.* **14**, 3153-3159, (2014).

70   Green, M. A., Ho-Baillie, A. & Snaith, H. J. The emergence of perovskite solar cells. *Nature Photon.* **8**, 506-514, (2014).

71   Snaith, H. J. Perovskites: The emergence of a new era for low-cost, high-efficiency solar cells. *J. Phys. Chem. Lett.* **4**, 3623-3630, (2013).

72   Xing, G. *et al.* Low-temperature solution-processed wavelength-tunable perovskites for lasing. *Nature Mater.* **13**, 476-480, (2014).

73   Deschler, F. *et al.* High photoluminescence efficiency and optically pumped lasing in solution-processed mixed halide perovskite semiconductors. *J. Phys. Chem. Lett.* **5**, 1421-1426, (2014).

74   Stranks, S. D. *et al.* Enhanced amplified spontaneous emission in perovskites using a flexible cholesteric liquid crystal reflector. *Nano Lett.* **15**, 4935-4941, (2015).

75   Zhu, H. *et al.* Lead halide perovskite nanowire lasers with low lasing thresholds and high quality factors. *Nature Mater.* **14**, 636-642, (2015).

76   Xing, J. *et al.* Vapor phase synthesis of organometal halide perovskite nanowires for tunable room-temperature nanolasers. *Nano Lett.* **15**, 4571-4577, (2015).

77   Niu, G., Guo, X. & Wang, L. Review of recent progress in chemical stability of perovskite solar cells. *J. Mater. Chem. A* **3**, 8970-8980, (2015).

78   Conings, B. *et al.* Intrinsic thermal instability of methylammonium lead trihalide perovskite. *Adv. Energy Mater.* **5**, 1500477, (2015).

79   Lee, J.-W. *et al.* Formamidinium and cesium hybridization for photo- and moisture-stable perovskite solar cell. *Adv. Energy Mater.* **5**, 1501310, (2015).

80   Nedelcu, G. *et al.* Fast anion-exchange in highly luminescent nanocrystals of cesium lead halide perovskites ($CsPbX_3$, X = Cl, Br, I). *Nano Lett.* **15**, 5635-5640, (2015).

81   Protesescu, L. *et al.* Nanocrystals of cesium lead halide perovskites (CsPbX, X = Cl, Br, and I): Novel optoelectronic materials showing bright emission with wide color gamut. *Nano Lett.* **15**, 3692–3696, (2015).

82   Wang, Y. *et al.* All-inorganic colloidal perovskite quantum dots: A new class of lasing materials with favorable characteristics. *Adv. Mater.* **27**, 7101–7108, (2015).

83   Yakunin, S. *et al.* Low-threshold amplified spontaneous emission and lasing from colloidal nanocrystals of caesium lead halide perovskites. *Nature Comm.* **6**, (2015).

84   Zhang, D., Eaton, S. W., Yu, Y., Dou, L. & Yang, P. Solution-phase synthesis of cesium lead halide perovskite nanowires. *J. Am. Chem. Soc.* **137**, 9230-9233, (2015).

85   Eaton, S. W. *et al.* Lasing in robust cesium lead halide perovskite nanowires. *Proc. Natl. Acad. Sci. U. S. A.* **In Press**, (2016).

86   Zhang, T. & Shan, F. Development and application of surface plasmon polaritons on optical amplification. *J. Nanomater.* **2014**, 16, (2014).

87   Berini, P. & De Leon, I. Surface plasmon-polariton amplifiers and lasers. *Nature Photon.* **6**, 16-24, (2012).

88   Khurgin, J. B. How to deal with the loss in plasmonics and metamaterials. *Nature Nanotechnol.* **10**, 2-6, (2015).

89   Maslov, A. V. & Ning, C. Z. Size reduction of a semiconductor nanowire laser by using metal coating. **6468**, 64680I-64680I-64687, (2007).

90   Oulton, R. F. Surface plasmon lasers: Sources of nanoscopic light. *Mater. Today* **15**, 26-34, (2012).

91   Oulton, R. F., Sorger, V. J., Genov, D. A., Pile, D. F. P. & Zhang, X. A hybrid plasmonic waveguide for subwavelength confinement and long-range propagation. *Nature Photon.* **2**, 496-500, (2008).

92   Oulton, R. F. *et al.* Plasmon lasers at deep subwavelength scale. *Nature* **461**, 629-632, (2009).

93   Lu, Y.-J. *et al.* Plasmonic nanolaser using epitaxially grown silver film. *Science* **337**, 450-453, (2012).

94   Sidiropoulos, T. P. H. *et al.* Ultrafast plasmonic nanowire lasers near the surface plasmon frequency. *Nature Phys.* **10**, 870-876, (2014).

95   Wu, X. *et al.* Hybrid photon-plasmon nanowire lasers. *Nano Lett.* **13**, 5654-5659, (2013).

96   Duan, X., Huang, Y., Agarwal, R. & Lieber, C. M. Single-nanowire electrically driven lasers. *Nature* **421**, 241-245, (2003).

97   Hill, M. T. *et al.* Lasing in metallic-coated nanocavities. *Nature Photon.* **1**, 589-594, (2007).

98   Ding, K. & Ning, C. Z. Fabrication challenges of electrical injection metallic cavity semiconductor nanolasers. *Semicond. Sci. Technol.* **28**, 124002, (2013).

99   Ding, K. *et al.* Room-temperature continuous wave lasing in deep-subwavelength metallic cavities under electrical injection. *Phys. Rev. B: Condens. Matter* **85**, 041301, (2012).

100   Ding, K. *et al.* Record performance of electrical injection sub-wavelength metallic-cavity semiconductor lasers at room temperature. *Opt. Express* **21**, 4728-4733, (2013).

101   Ding, K. *et al.* An electrical injection metallic cavity nanolaser with azimuthal polarization. *Appl. Phys. Lett.* **102**, 041110, (2013).

102   Li, K. H., Liu, X., Wang, Q., Zhao, S. & Mi, Z. Ultralow-threshold electrically injected AlGaN nanowire ultraviolet lasers on Si operating at low temperature. *Nature Nanotechnol.* **10**, 140-144, (2015).

103   Zhao, S. *et al.* An electrically injected AlGaN nanowire laser operating in the ultraviolet-C band. *Appl. Phys. Lett.* **107**, 043101, (2015).

GLOSSARY

Stimulated emission

The emission of a photon through the relaxation of an excited electronic state that is triggered (stimulated) by an incident photon; the emitted photon shares phase, polarization, and direction with the incident photon.

Absorption

The optical process by which a photon with proper energy and polarization disappears and causes an excitation of an electron to the higher energy state.

Lasing

The action of a device that enables light amplification by stimulated emission of radiation.

Optical Gain

A measure of the ability of a material to increase the optical power through the transfer of energy from a medium into the electromagnetic field, or the logarithm of the ratio of outgoing power to incoming power per unit length.

Optical fiber

A thin structure made of a core of high refractive index material and cladding layer of low index of refraction that can guide light along its length, which can be used for the transmission of signal across great distances with relatively small losses in signal.

LIDAR

An acronym that stands for light detection and ranging that employs a pulsed laser to generate 3D topography maps.

Vertical-cavity surface emitting lasers (VCSELs)

A type of monolithic semiconductor laser diodes with light emission perpendicular to the surface of the plane of the semiconductor wafer.

Microdisk laser

A type of laser in which the gain medium is a micron-sized disc, typically suspended above the supporting substrate by a stem.

Photonic crystal

An artificial structure made of materials with periodically high and low indices of refraction; such structures can have photonic band structures analogous to electronic band structures in regular solid crystals.

Semiconductor

A type of material that has a conductivity in between insulators and metals, and upon excitation, an electron and hole are generated, which can recombine to emit a photon.

Nanowire

A thin wire with a diameter on the length scale of 10^{-9} meters (nm).

Compositional wavelength tunability

Changing the wavelength of emission by changing the composition to control energy levels of the material.

Optoelectronic devices

Devices which utilize both electronic and optical processes for their operation.

Vapor-liquid-solid growth

        A growth mechanism for growing solid nanostructures such as nanowires by chemical vapor deposition in which a chemical vapor precursor dissolves in a liquid droplet that is often metallic.

Extended defects

        Imperfections in the crystal lattice that extend beyond a point, which are often associated with states that enable non-radiative recombination of charge carriers or excitons.

Top-down

        Referring to an approach to fabricating nanostructures beginning with a macroscale crystal to produce nanostructures, typically through lithography and etching.

Bottom-up

        Referring to an approach to creating nanostructures beginning with chemical precursors to grow nanostructures.

Near-field scanning optical microscopy (NSOM)

        A microscopy technique in which the detector is placed a small distance (less than a wavelength of light) from the sample surface and the sample image resolution is limited by the dimensions of the detector aperture rather than the wavelength of the light used.

Photoluminescence

        Light emission from a material caused by recombination of an electron and hole after excitation by an incident photon; also referred to as "emission" from the relaxation of an excited state.

Lasing threshold

        The degree of excitation at which the light emission in a device becomes dominated by stimulated emission instead of spontaneous emission; at this level of excitation, gain and loss from the laser cavity are in balance.

Far-field

The region far from source of electromagnetic radiation in which near-field phenomena are not observed, typically at a distance much larger than the wavelength concerned.

Fabry–Pérot cavity

A type of laser cavity that can be represented as two flat and parallel reflective surfaces; nanowire cavities are generally considered examples of Fabry–Pérot cavities, where each end facet behaves as a localized scatter, rather than extended flat surfaces.

Optical feedback

A process that occurs when the optical field from the gain medium is bounced back and forth in a structure or cavity, such that photon can be retained for a longer time.

Confinement factor

A factor that describes the effective overlap between a gain medium and an optical field or mode; the ratio of the gain experienced by a mode to that experienced by a plane wave in an infinitely large uniform medium.

Mirror loss

Losses that occur due to imperfect reflectivity on either end of a laser cavity such as in a Fabry–Pérot cavity.

Propagation loss

Losses of a signal transmitted within a medium when a wave propagates from one point to another.

Reflection coefficients

Quantity used to quantify the amount of reflection of wave at a material interface as a fraction of incident wave.

Resonator

An object, device, or system that can support modes of a wave at certain specific frequencies of that wave.

Modes

The spatial profiles of the allowed resonances of a wave in a resonator or optical fiber.

Absorption cross-section

A quantity describing the likelihood of the absorption of an incident photon or other energetic particle on an object.

Trap state

An energetic state that tends to trap electrons or holes in a material which are often associated with increased non-radiative recombination.

Amplified spontaneous emission (ASE)

A process by which spontaneous emission (photoluminescence) is amplified in a gain medium.

Electron−hole recombination

The simultaneous disappearance of an electron and hole, which results in the radiative emission of a photon or non-radiative dissipation of energy within the material.

Photoluminescence quantum efficiency

The ratio of the photons emitted from a material to the photons incident on (external) or absorbed by the material (internal).

Ring resonators

A resonator in which the cavity is in the shape of a ring.

Q-factors

Parameters describing the quality of a resonator cavity in terms of energy loss; it is directly proportional to the ratio of energy stored to energy lost per cycle.

Cleaved-coupled cavity

A laser cavity composed of two Fabry–Pérot cavities coupled through a narrow air gap.

Finite element method

A numerical method for approximating solutions to differential equations with boundary values by subdividing the whole object into finite elements.

Finite-difference time-domain

A numerical simulation method for approximating to solutions to systems of partial differential equations by sub-dividing time into small discrete intervals.

Surface plasmon polaritons (SPP)

Excited electromagnetic waves coupled to the excitation of motions of charged particles that propagate along a metal-dielectric interface.

Dielectric medium/material

A material that has insulating properties but that can be polarized by an applied electric field.

Plasmonic

Referring to a plasmon, which is a quanta of plasma oscillation, often in metals where electrons can be coupled to photons.

Injection layer

A highly doped layer used to inject charges into an electrically pumped laser.

Superlinear

Describing a trend that grows more quickly than a linear function with a dependent variable.